ChemPubSoc Europe

DOI: 10.1002/chem.201404083

CHEMISTRY
A European Journal
Full Paper

Tautomerism

NMR Studies of Active-Site Properties of Human Carbonic Anhydrase II by Using ^{15}N-Labeled 4-Methylimidazole as a Local Probe and Histidine Hydrogen-Bond Correlations

Ilya G. Shenderovich,*[a] Stepan B. Lesnichin,[b] Chingkuang Tu,[c] David N. Silverman,*[c] Peter M. Tolstoy,[d] Gleb S. Denisov,[e] and Hans-Heinrich Limbach*[b]

Abstract: By using a combination of liquid and solid-state NMR spectroscopy, ^{15}N-labeled 4-methylimidazole (4-MI) as a local probe of the environment has been studied: 1) in the polar, wet Freon CDF_3/CDF_2Cl down to 130 K, 2) in water at pH 12, and 3) in solid samples of the mutant H64A of human carbonic anhydrase II (HCA II). In the latter, the active-site His64 residue is replaced by alanine; the catalytic activity is, however, rescued by the presence of 4-MI. For the Freon solution, it is demonstrated that addition of water molecules not only catalyzes proton tautomerism but also lifts its quasidegeneracy. The possible hydrogen-bond clusters formed and the mechanism of the tautomerism are discussed. Information about the imidazole hydrogen-bond geometries is obtained by establishing a correlation between published ^{1}H and ^{15}N chemical shifts of the imidazole rings of histidines in proteins. This correlation is useful to distinguish histidines embedded in the interior of proteins and those at the surface, embedded in water. Moreover, evidence is obtained that the hydrogen-bond geometries of His64 in the active site of HCA II and of 4-MI in H64A HCA II are similar. Finally, the degeneracy of the rapid tautomerism of the neutral imidazole ring His64 reported by Shimahara et al. (*J. Biol. Chem.* **2007**, *282*, 9646) can be explained with a wet, polar, nonaqueous active-site conformation in the inward conformation, similar to the properties of 4-MI in the Freon solution. The biological implications for the enzyme mechanism are discussed.

Introduction

Human carbonic anhydrase (HCA II) is an ubiquitous enzyme that catalyzes the reversible hydration of CO_2 to produce HCO_3^- and a proton.[1–4] It contains in the active site an essential triple-histidine-liganded zinc ion, to which either a water molecule or the corresponding hydroxide base is bound. As illustrated in Scheme 1, the central catalytic step of the hydration reaction is the nucleophilic attack in state **1** of zinc-bound hydroxide onto CO_2 to form bicarbonate HCO_3^-, which then dissociates from the metal.[2,3,5]

A water molecule then binds to the zinc ion, which leads to state **2**. The rate-limiting step for the maximal velocity of the enzyme reaction is the following proton transfer from zinc-bound water in state **2** via several water molecules to the imidazole ring B of a histidine side chain (His64).[1–3,6,7] Ring B is located about 7 Å away from the zinc ion, as illustrated by the

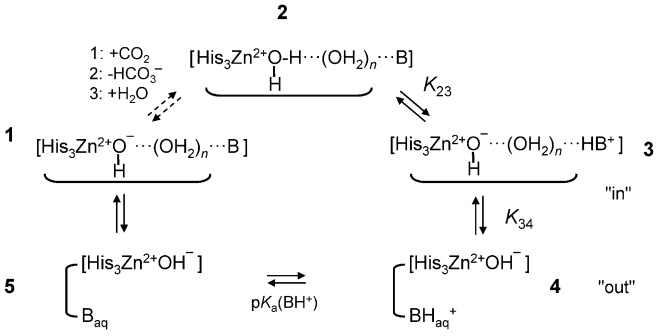

Scheme 1. General reaction scheme of human carbonic anhydrase II (HCA II). "B" stands for the base histidine 64 (His64). For further information, see the main text.

[a] *Dr. I. G. Shenderovich*
University of Regensburg
Universitätsstrasse 31, 93053 Regensburg (Germany)
E-mail: Ilya.Shenderovich@chemie.uni-regensburg.de

[b] *Dr. S. B. Lesnichin, Prof. Dr. H.-H. Limbach*
Institut für Chemie und Biochemie, Freie Universität Berlin
Takustrasse 3, 14195 Berlin (Germany)
E-mail: limbach@chemie.fu-berlin.de

[c] *Dr. C. Tu, Prof. Dr. D. N. Silverman*
Departments of Pharmacology and Therapeutics, and
Biochemistry and Molecular Biology, University of Florida
College of Medicine, Gainesville, Florida 32610 (USA)
E-mail: silvrmn@ufl.edu

[d] *Dr. P. M. Tolstoy*
Department of Chemistry, St. Petersburg State University
Universitetskij pr. 26, 198504, St. Petersburg (Russian Federation)

[e] *Prof. Dr. G. S. Denisov*
Institute of Physics, St. Petersburg State University
198504 St. Petersburg (Russian Federation)

Supporting information for this article is available on the WWW under http://dx.doi.org/10.1002/chem.201404083.

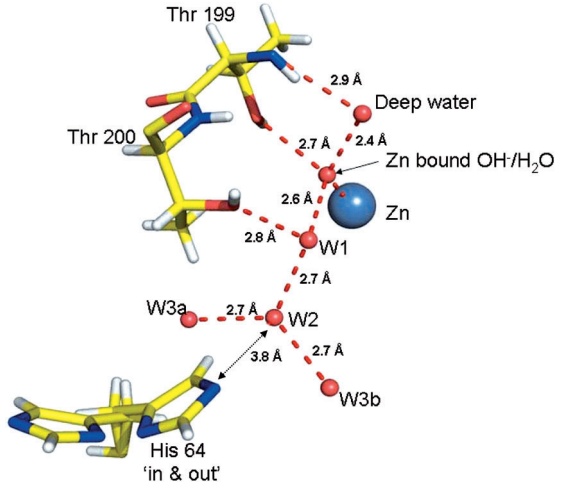

Figure 1. X-ray crystallographic structure of the active site of HCA II according to Avvaru et al.[9] showing the ordered water network. The red spheres represent the oxygen atoms of water molecules, and the dotted lines represent presumed hydrogen bonds.

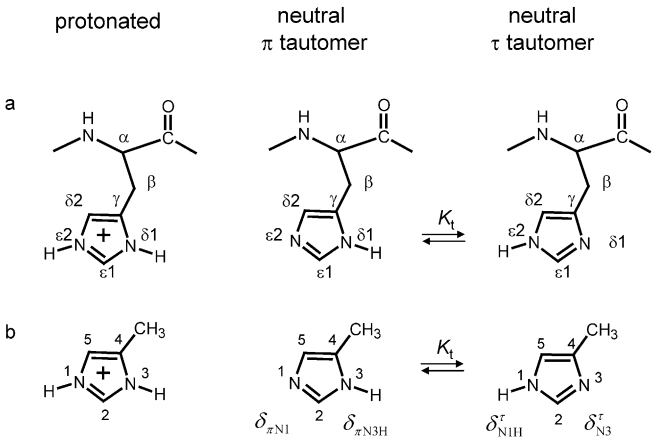

Scheme 2. Chemical structures of: a) protonated and neutral histidine, and b) 4-methylimidazole (4-MI). Various atom-numbering schemes have been used for the imidazole derivatives previously.[90] Whereas for small imidazoles, such as 4-MI, the normal numbers 1–5 are used, the histidine imidazole nitrogen atoms have previously been labeled as τ (tele, far) and π (near) from the side chain. Greek letters are often used for referring to the distance to the main chain. For the comparison of 4-MI with His64, we will use here the normal numbering scheme. When the imidazole ring is neutral, the proton can be located either on the N1 or the N3 atom. The two tautomers formed are generally named as the π or the τ tautomer. Their ratio is characterized by the equilibrium constant K_t.

X-ray crystal structure of the active site,[2,8,9] depicted in Figure 1.

It has been observed that ring B can form an inward and an outward conformation,[8,10,11] consistent with the suggestion that the proton is received in the inward conformation **3** and that a conformational change occurs to the outward conformation **4**, which enables proton transfer to the aqueous phase (state **5**). The cycle is completed after forming again state **1**. However, to our knowledge, it has not yet been shown that the intramolecular proton transfer requires the inward conformation and that the proton transfer to the buffer in solution requires the outward conformation of His64.

The important role of His64 was suggested by Steiner et al.[1a] and demonstrated by Silverman and co-workers,[12,13] who observed that replacement of His64 by Ala in the mutant H64A HCA II reduces dramatically the catalytic activity; however, the latter is chemically rescued to a near wild-type (WT) level by the incorporation of 4-methylimidazole (4-MI, Scheme 2b) or other heterocyclic nitrogen bases into the active site. X-ray crystallographic studies[14,15] have shown that 4-MI preferentially binds to the active site, where it takes the position of His64 in the inward or the outward conformation. This active-site binding has been confirmed by ^{1}H NMR relaxometry by substitution of the Zn^{II} ion in H64A HCA II by a paramagnetic Co^{II} ion, from which binding constants were also obtained.[16] In addition, further binding sites of 4-MI located near several amino acid residues of H64A HCA II have been identified.[15]

The proton-transfer kinetics is strongly influenced by the basicity of the added bases.[7,10,12] As illustrated in Scheme 2b, the imidazole rings of histidines or other 4(5)-substituted histidines, such as 4-MI, are either protonated or uncharged in the vicinity of the physiological pH value. At very high pH values, there is a third ionization state, the imidazolate anion, which we do not consider here further. In the neutral state, both the π and the τ tautomer can be formed, depending on the protonation state of the ammonium group in the case of free histidine.

The acid–base properties of histidine[17] and histidine side chains[18–20] in aqueous solution have been studied by using ^{15}N NMR spectroscopy. Blomberg et al.[17] found a pK_a value of 7.2 for the imidazole ring of histidine in aqueous solution. In seminal ^{1}H and ^{15}N NMR studies of His64 in HCA II, Campbell et al.[21] and, more recently, Shimahara et al.[20] found similar values for His64, although these were averaged over the inward and outward conformations. Whereas this result is plausible for the outward conformation, in which the imidazole ring is embedded in water, the question of the equilibrium constant K_{23} in Scheme 1, that is, of the basicity of His64 in the inward conformation, is still under debate.

Several authors have performed various calculations on the proton transfer from zinc-bound water to His64.[10,11,22–27] Elstner et al.[24] have calculated for an active-site model of HCA II only little free energy changes for proton transfer from zinc-bound water to imidazole through a chain of two water molecules. By using a hybrid QM/MM approach, Warshel and coworkers[26,27] have computed an uphill or a downhill reaction for different carbonic anhydrases depending on the type of enzyme. Maupin et al.[10,22] found in a similar way that the free energy increases for the protonation step from **2** to **3** in Scheme 1 but decreases for the following conformational change to **4**, which renders the proton transfer from zinc-bound water to bulk water almost isoenergetic. Finally, by using a small-molecule model system, some of us have shown that, if zinc-bound water forms a direct hydrogen bond to a pyridine-type nitrogen atom, the proton is located closer to the nitrogen atom than to the oxygen atom.[28]

Another puzzling property of His64 in HCA II has been revealed by Shimahara et al.[20] Whereas the equilibrium con-

stants of tautomerism, K_t (Scheme 2), of most histidine imidazole rings of HCA II are larger than 3, similar to the value of 4 found for the histidine monomer in aqueous solution at high pH values,[17] His64 exhibits a value of 1. Again, this value is averaged over the inward and outward conformations. This astonishing result has been discussed as useful for the catalytic activity,[20] but how this is achieved by the enzyme is not understood to date to our knowledge.

By comparison of small molecular active-site models with cofactors in aminotransferases by using a combination of low-temperature ^1H and ^{15}N liquid-state and ^{15}N solid-state NMR spectroscopy, some of us have shown that active-site acid–base interactions are better modeled by using polar aprotic solvents exhibiting dielectric constants of around 30, rather than aqueous solutions.[29–32] Thus, we suspected that the puzzling behavior of His64 in HCA II might be related to an aprotic polar environment, in spite of the presence of some water molecules in the active site. However, experimental modeling of the environment of an important side chain such as His64 is not a trivial task, because histidine itself is not soluble in organic solvents.

Herein, we propose to solve the His64 problem of HCA II by exploiting the finding of Silverman and co-workers[12] that 4-MI (Scheme 2) rescues the catalysis of the mutant H64A HCA II, in which the histidine in position 64 has been substituted for alanine. This finding provided us with the unique opportunity to conduct a comparative study of ^{15}N-labeled 4-MI embedded both in the lyophilized mutant enzyme by using ^{15}N solid-state NMR spectroscopy and in the polar aprotic solvent CDF_3/CDF_2Cl by using low-temperature ^1H/^{15}N NMR spectroscopy.[33–35] This solvent can adopt some water molecules, which have been shown to form OHN hydrogen bonds to heterocyclic pyridines down to 100 K.[36] This technique allowed us to access the slow proton and hydrogen-bond exchange regimes of 4-MI and to study the effect of water molecules on these exchange processes. On the other hand, solid-state ^{15}N NMR spectroscopy has been established as a reliable method to study protonation states and proton dynamics of nitrogen-containing heterocycles in various crystalline and amorphous solids.[37–42] An X-ray crystal structure of 4-MI has not yet been reported to our knowledge; however, an early study of the neat liquid by Zimmermann, the PhD supervisor for one of us (H.H.L.), had shown that 4-MI forms linear hydrogen-bonded chains.[43]

In order to characterize the basicity of His64 in the inward conformation, we have studied the ^{15}N solid-state NMR spectra of ^{15}N-labeled 4-MI after incorporation into wild-type HCA II, Zn^{II} H64A HCA II, and also the cobalt-substituted site-specific mutant, Co^{II} H64A HCA II for comparison. This substitution does not affect remarkably the efficiency of the catalytic reaction but presumably results in some structural changes of the active site.[16,44,45]

Finally, we have tackled the problem of how the ^1H and ^{15}N chemical shifts of imidazole rings in various environments provide insight into the geometries of the hydrogen bonds in which the imidazole nitrogen atoms are involved, generally with oxygen atoms. Previously, we have observed correlations between the ^1H and ^{15}N NMR chemical shifts and the geometries of OHN hydrogen bonds formed by pyridine derivatives.[46,47] The structural chemical-shift changes mean that these correlations need to be adapted for use with imidazole rings. Moreover, only data from systems exhibiting slow hydrogen-bond and proton exchanges can be used. These requirements are often met for solid-state samples. Therefore, we have assembled the ^1H and ^{15}N NMR chemical shifts of imidazole rings in proteins published by different authors. Indeed, we observe OHN hydrogen-bond correlations that might be useful in the future to obtain information about the hydrogen-bond geometries of histidine side chains.

This paper is organized as follows. After the Experimental Section, we describe the results of our NMR studies of ^{15}N-enriched 4-MI 1) dissolved in the wet Freon mixture CDF_3/CDF_2Cl and in the polycrystalline state and 2) embedded in zinc- and cobalt-containing wild-type HCA II and its mutant H64A HCA II. We then describe a novel ^1H–^{15}N hydrogen-bond chemical-shift correlation for the imidazole rings of histidines, which allows us to obtain hydrogen-bond geometries from these data. Finally, the results obtained will be discussed with respect to their biological implications.

Experimental Section

Compounds

In this study, we used 4-methylimidazole (4-MI), 4-methylimidazole-$^{15}N_2$ (4-MI-$^{15}N_2$), and 4-methylimidazole-2-^{13}C,$^{15}N_2$ (4-MI-2-^{13}C,$^{15}N_2$). Solid 4-MI was obtained as a solid with a melting point of 44–45 °C from Sigma–Aldrich, and the labeled compounds were synthesized by modification of the synthesis of 4-MI.[48] In the following paragraph, we describe only the synthesis of 4-MI-2-^{13}C,$^{15}N_2$.

Diluted sulfuric acid (3 drops of concentrated sulfuric acid in 2 mL of water) was added dropwise to a solution of $(^{15}NH_4)_2SO_4$ (1.28 g, 9.5 mmol) in water (6.6 mL) until a pH value of 2 was reached. The mixture was then heated up to 80 °C. A mixture of ^{13}C-labeled formaldehyde (1 g, 20% solution in water, 6.4 mmol, 99% ^{13}C, Sigma–Aldrich) or of the unlabeled isotopologue with methylglyoxal (1.09 g, 6 mmol) was added dropwise to the solution. The pH value was monitored and kept at 2 during the reaction, with adjustment with addition of $^{15}NH_3$ (20% in water prepared as described previously[38]) if necessary. After 2.5 h, a small amount of ethanol was added to the brown mixture. This was followed by solvent evaporation under reduced pressure. A 20% $^{15}NH_3$ solution in water (5 mL) and isobutanol (7 mL) were added to the brown solid residue, and the mixture was stirred at room temperature. The upper layer was collected, and fresh isobutanol was added to the residue, with subsequent continued stirring at room temperature. The procedure was repeated three times. A pellet of KOH was added, and the extraction procedure was continued with control by NMR spectroscopy and fluorescence measurements at 366 nm. The isobutanol phases were then unified, and the solvent was evaporated to yield a brown oily residue. There was only small quantity of the latter so we could not perform an ordinary distillation, only a ball-tube distillation (0.8 mbar, 80–130 °C). The product (0.38 g) was obtained as a clear light yellow but very viscous oil, which indicated the presence of a small quantity of impurities. The ^1H and ^{13}C NMR spectra agree, however, with the published data.[49]

The Freon mixture CDF_3/CDF_2Cl (99.6% D), used as the NMR solvent down to 100 K, was synthesized as described previously by some of us.[50] Liquid-state NMR samples were equipped with a teflon needle valve (Wilmad, Buena, N.Y.) and prepared by using vacuum methods.[33]

The site-specific mutant H64A HCA II of human carbonic anhydrase II was expressed in *Escherichia coli* as described by Taoka et al.[51] Cobalt substitution for zinc was done as described by Elder et al.[16] In summary, the enzyme was placed in 0.25 M 2-[4-(2-hydroxyethyl)-1-piperazinyl]ethansulfonic acid (HEPES) buffer at pH 7.3 containing 0.5 M of the chelator dipicolinic acid, and the mixture was stirred for 4 h at 4 °C. The sample was dialyzed extensively against 1 mM tris(hydroxymethyl)aminomethane (Tris) at pH 8.0, after which cobalt sulfate was added at a final concentration of 1 mM. Finally, the sample was dialyzed against 1 mM Tris at pH 8.0 to remove excess metal and chelator. Metal substitution in the enzyme was verified by the visible absorption spectrum as previously described.[16] Samples of wild-type and site-specific mutants of HCA II loaded with ^{15}N,^{13}C-enriched 4-MI were prepared by dissolving the enzymes in water at the desired pH value, adding one equivalent of 4-MI, and subsequent lyophilization. Under these conditions, all of the 4-MI is bound to the H64A HCA II.[15,16] Note that the dialysis could not be performed after addition of 4-MI because the latter would be removed from the sample.

NMR spectroscopy

Liquid-state NMR spectra were recorded on a Bruker AMX-500 instrument operating at 11.7 Tesla (500.13 MHz for ^1H, 50.68 MHz for ^{15}N). A Eurothermic variable temperature unit was used to adjust the temperatures with an accuracy of ± 1 K. The ^{15}N chemical shifts of the Freon samples were measured with respect to internal ^{15}N-labeled 2,6-di(*tert*-butyl)-4-diethylaminopyridine,[52] which resonates at $\delta = 277$ ppm with respect to liquid $^{15}NH_3$ at 25 °C.

Solid-state NMR spectra were recorded on Varian Infinity Plus 300 MHz (7 T) and 600 MHz (14 T) solid-state NMR spectrometers under magic angle spinning (MAS) conditions by using spinning rates of about 10 kHz with a standard ^{15}N $\{^1H\}$ cross-polarization (CP) NMR pulse sequence with a cross-polarization contact time of 3 ms. This technique may not provide a correct ratio for the integral intensities of the two ^{15}N peaks of 4-MI, so a *z* filter was used when necessary, through which the ^{15}N magnetization created by cross-polarization was placed for 1.0 s along the direction of the external magnetic field to allow for ^{15}N spin diffusion to occur among two nitrogen atoms of the same 4-MI molecule.[53] The 90° pulse width was about 8 μs, and the recycle times were 20 s. The number of scans per spectrum was between 10000 and 40000. All parameters used to obtain the NMR spectra reported in this study are assembled in the Supporting Information.

We used ^{15}N-labeled solid glycine as the primary external chemical-shift reference; it resonates at $\delta = 6.5$ ppm with respect to solid $^{15}NH_4Cl$ and at $\delta = 47$ ppm with respect to liquid $^{15}NH_3$ at 25 °C. All ^{15}N chemical shifts reported herein were finally converted into the ammonia scale.[54–56]

Results

^{15}N NMR spectroscopy of 4-methylimidazole-2-^{13}C,$^{15}N_2$ in water at pH 12, in wet CDF_3/CDF_2Cl, and in the solid state

The ^{15}N NMR spectra of 4-MI-2-^{13}C,$^{15}N_2$ obtained in this study under various conditions are depicted in Figure 2.

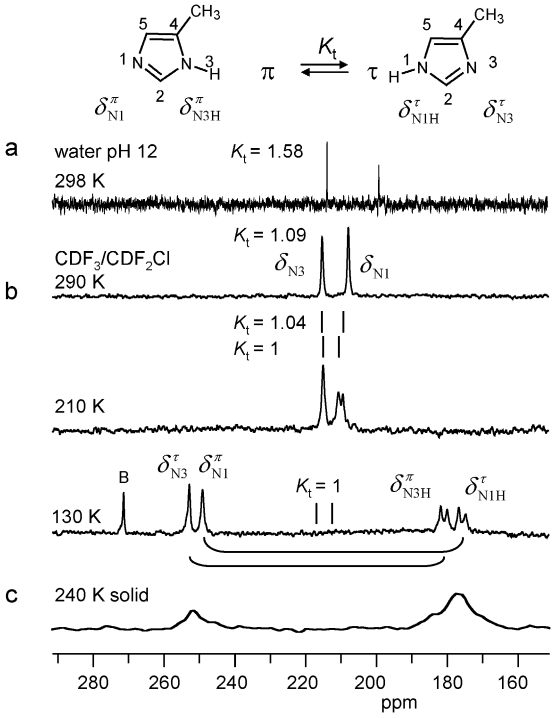

Figure 2. a) ^{15}N NMR spectrum (50.68 MHz INEPT) at 299 K of 4-MI at natural abundance dissolved in D_2O at pH 12. b) Variable-temperature 50.68 MHz ^{15}N NMR spectra of 4-MI-2-^{13}C,$^{15}N_2$ dissolved in wet CDF_3/CDF_2Cl. A small amount of 2,6-di(*tert*-butyl)-4-diethylaminopyridine (labeled as "B") was used as an internal primary reference. c) ^{15}N CP MAS NMR spectrum of bulk solid 4-MI-$^{15}N_2$ at 60.6 MHz. For the conversion of different ^{15}N chemical-shift scales, see Table S1 in the Supporting Information.

The chemical shifts obtained are assembled in Table 1. At room temperature, in the liquid-state study, two signals are observed for the N1 and N3 atoms, averaged over the π and τ tautomers that exchange rapidly within the NMR timescale. The chemical-shift difference, $\delta_{N3}-\delta_{N1}$, depends on the intrinsic chemical shifts and the equilibrium constant of tautomerism, K_t, as will be discussed in detail below. Previously, Roberts and co-workers[57] and Chen et al.[58] had observed chemical-shift differences of 5.5 and 5.8 ppm with $CDCl_3$ as solvent, of 8.9 with DMSO,[58] and of 8.4 ppm in neutral aqueous solution at pH 7[57] (Table 1). The assignment of the high-field peak to the N1 atom and the low-field peak to the N3 atom was justified[57] because the high-field signal was split into a triplet (J(N1,H2)≅J(N1,H5) = 8.7 Hz) and the low-field signal into a doublet (J(N3,H2) = 9.4 Hz).

In order to obtain the chemical-shift difference of neutral 4-MI in water, we measured the ^{15}N NMR spectrum in D_2O at pH 12, which is well above the pK_a value of 7.52.[59] As illustrated in Figure 2a, we observe a splitting of 14.6 ppm.

At this date, to our knowledge, the slow-exchange regime between the two tautomers has not yet been observed, so we performed low-temperature NMR experiments on 4-MI-2-^{13}C,$^{15}N_2$ dissolved in CDF_3/CDF_2Cl, which is liquid down to 100 K. We were astonished that we were able to record spectra at 130 K without solubility problems. A fairly well resolved spectrum was obtained, as illustrated in Figure 2b, containing

Table 1. ^{15}N NMR chemical shifts of 4-MI referenced to external $^{15}NH_3$ at 25 °C.[a]

Sample	Ref.	pH value	T [K]	δ ^{15}N [ppm]	
	herein		130	252.9 (δ^{τ}_{N3})	175.8 (δ^{τ}_{N1H})
	herein			249.2 (δ^{π}_{N1})	181.0 (δ^{π}_{N3H})
4-MI-$^{15}N_2$-^{13}C in Freon	herein	–	210	215.3 (δ_{N3})	215.7 (δ_{N1})
	herein			215.3 (δ_{N3})	215.5 (δ_{N1})
	herein		290	215.3 (δ_{N3})	208.0 (δ_{N1})
4-MI in $CDCl_3$	[57b]		298	216.0 (δ_{N3})	210.5 (δ_{N1})
4-MI in H_2O at pH 7	[57a]		298	213.1 (δ_{N3})	204.7 (δ_{N1})
4-MI in D_2O at pH 12	herein		299	212.3 (δ_{N3})	197.7 (δ_{N1})
4-MI in dimethylsulfoxide (DMSO)	[58]			218.0 (δ_{N3})	209.1 (δ_{N1})
4-MI in $CDCl_3$	[58]			214.9 (δ_{N3})	209.1 (δ_{N1})
4-MI bulk	herein	–	290	253 (δ_N)	177 (δ_{NH})
4-MI-$^{15}N_2$ in Zn^{II} WT HCA II	herein	7.8	240	–	173 (δ_{NH+})
4-MI-$^{15}N_2$ in Zn^{II}H64A HCA II	herein	5.8	240	–	173 (δ_{NH+})
4-MI-$^{15}N_2$ in Zn^{II}H64A HCA II	herein	7.8	240	253 (δ_N)	173 (δ_{NH})
4-MI-$^{15}N_2$ in Co^{II} WT HCA II	herein	7.8	240	–	173 (δ_{NH+})
4-MI-$^{15}N_2$ in Co^{II}H64A HCA II	herein	7.8	240	–	180 (δ_{NH+})

[a] δ (ref. NH_3, 25 °C) = δ (ref. solid NH_4Cl) + 40.5 ppm. δ (ref. NH_3, 25 °C) = δ (ref. 1 M HNO_3) + 377.5 ppm (Day et al.[19]).

four signals of equal intensity. The two high-field signals exhibit asymmetric doublets arising from coupling with the attached protons, whereas the low-field signals constitute singlets. The asymmetry arises from the interference of the ^1H–^{15}N dipolar couplings and the ^{15}N chemical-shift anisotropy combined with a reduced molecular mobility.[60] Owing to the short transverse relaxation times, further couplings to CH protons and the nitrogen–nitrogen couplings were not resolved. Clearly, the slow-exchange regime between the two tautomers was reached, and the mole fractions of both tautomers were the same within the margin of error, which indicated the equilibrium constant of tautomerism as $K_t = 1$.

For an internal reference standard, we added a small amount of the sterically hindered base 2,6-di(*tert*-butyl)-4-diethylaminopyridine,[52] which contributed a signal at $\delta =$ 271.5 ppm labeled as "B" in Figure 2. This signal was, however, observed only at 130 K because of unfavorable relaxation properties, which is typical for nonprotonated nitrogen atoms that are neither protonated nor hydrogen bonded.

When the temperature was increased, the lines broadened and disappeared into the baseline. However, we were surprised to observe already at 210 K two relatively sharp averaged signals, in which the lower-field signal clearly corresponds to the N3 atom and the higher-field signal to the N1 atom, as demonstrated by comparison with the spectrum at 290 K. The N1 signal is split into two components that are consistent with two different 4-MI environments exhibiting chemical-shift differences, $\delta_{N3}-\delta_{N1}$, of 4.4 and 5.6 ppm. However, the splitting disappears upon heating. Finally, we notice a small shift of all signals to higher field with increasing temperature.

In order that proton tautomerism produces a higher field N1 and a lower field N3 signal, one must assume the signal assignment and exchange pathways as depicted at the bottom of Figure 2b: that is, the N3 atom resonates at lower field both in the amino and in the imino form as compared with N1. Thus, we could then assign the two coupling constants $J^{\pi}(N3,H) = 92$ Hz and $J^{\tau}(N1,H) = 97$ Hz.

For comparison, in Figure 2c, the ^{15}N solid-state CP MAS NMR spectrum of 4-MI-$^{15}N_2$ is depicted. Two distinct imino and amino signals are observed, which indicates that the tautomeric exchange is quenched. Cross-polarization leads to a larger intensity of protonated nitrogen atoms than nonprotonated nitrogen atoms, so the magnetizations were stored for 1 s in the *z* direction for equilibration through spin diffusion, as mentioned above (*z* filter). This equilibration process was, however, not complete, and an intensity difference remained. The chemical shifts obtained are very similar to those found for the Freon study at 130 K, but the signals are too broad in order to resolve the contributions of the π and τ tautomers. On the other hand, the chemical-shift comparison indicates that, most probably, both tautomers are formed with similar mole fractions.

Equilibrium constants of proton tautomerism of 4-MI in wet CDF_3/CDF_2Cl

We know the chemical shifts in the slow-exchange regime of tautomerism, so we are able to obtain equilibrium constants of tautomerism from the observed splittings in the fast-exchange range.

The average chemical shifts of the N1 and N3 atoms are given by Equations (1).

$$\delta_{N3} = \frac{1}{1+K_t}\delta^{\pi}_{N3H} + \frac{K_t}{1+K_t}\delta^{\tau}_{N3} \qquad (1)$$

$$\delta_{N1} = \frac{1}{1+K_t}\delta^{\pi}_{N1} + \frac{K_t}{1+K_t}\delta^{\tau}_{N1H}$$

From these equations, Equation (2) follows in a straightforward way.

$$K_t = \frac{(\delta_{N3}-\delta_{N1}) + (\delta^{\pi}_{N1}-\delta^{\pi}_{N3H})}{(\delta^{\tau}_{N3}-\delta^{\tau}_{N1H}) - (\delta_{N3}-\delta_{N1})} \qquad (2)$$

By assuming that $\delta^{\pi}_{N1} - \delta^{\pi}_{N3H}$ and $\delta^{\tau}_{N3} - \delta^{\tau}_{N1H}$ are independent of the temperature and the solvent, we are able to calculate the equilibrium constants, K_t, from the values of $\delta_{N3}-\delta_{N1}$ obtained herein and reported for 4-MI in the literature. The results are assembled in Table 2. We have added the value of 1.5 reported by Wasylishen and Tomlinson[61] for 4-MI in water obtained from the ^3J(C5,H2) constant based on the corresponding value for 1-methylimidazole. This value agrees well with our value of 1.58 obtained for pH 12 from the observed value of $\delta_{N3}-\delta_{N1} = 14.6$ ppm (Figure 2a). These results will be discussed later.

Table 2. Equilibrium constants of tautomerism, K_t, of 4-MI in different solvents calculated from the difference between the ^{15}N chemical shifts of the N1 and N3 atoms.

Solvent	Ref.	T [K]	$(\delta_{N3}-\delta_{N1})$ [ppm]	K_t[a]
	herein	210	4.4	1.00
Freon	herein	210	5.6	1.04
	herein	290	7.3	1.09
$CDCl_3$	[57b]	298	5.5	1.03
$CDCl_3$	[58]	296	5.8	1.04
DMSO	[58]	296	8.9	1.13
H_2O at high pH value	[57a]	298	8.4	1.11
D_2O at pH 12	herein		14.6	1.58
H_2O at pH 11	[61]	303	–	1.5[b]

[a] Calculated by using Equation (2) and the values $\delta^{\pi}_{N1}+\delta^{\pi}_{N3H}=68.2$ ppm and $\delta^{\tau}_{N3}+\delta^{\tau}_{N1H}=77.1$ ppm, taken from Table 1. [b] Calculated from ^3J(C5,H2).

^{1}H NMR spectroscopy of 4-methylimidazole-2-^{13}C,$^{15}N_2$ in wet CDF_3/CDF_2Cl

In order to obtain more information about the mechanism of the proton tautomerism of 4-MI, we measured the corresponding ^{1}H NMR spectra, which are depicted in Figure 3. We observed a broadened singlet at $\delta=15.2$ ppm at 130 K, which is typical for a hydrogen bond of moderate strength. We assign this signal to the protons in the NHN hydrogen bonds between different 4-MI molecules. The signal stems from the NH protons of both the π and the τ tautomers and should exhibit the ^{1}H–^{15}N coupling observed by ^{15}N NMR spectroscopy. However, because of a small chemical-shift difference and fast transverse relaxation, these couplings are obscured. The characteristic doublet of the H2 atom arising from coupling with the C2 atom ($J=208$ Hz) appears at $\delta=7.75$ ppm. Each signal component is further split into a triplet by coupling with the two ^{15}N atoms ($J\approx9.5$ Hz), as revealed at higher temperatures. The H5 atom contributes two signals at $\delta=6.93$ and 6.85 ppm. We assign these two signals to the two tautomers because only a coalesced line arising from the interconversion of both tautomers is observed at 150 K. The residual solvent protons give rise to a triplet (CHF_2Cl) at $\delta=7.18$ ppm and a quartet (CHF_3) at $\delta=6.5$ ppm,[50] as illustrated by the inset spectrum. The aromatic proton signal of the added base, 2,6-di(*tert*-butyl)-4-diethylaminopyridine (labeled as "B") appears at around $\delta=6.5$ ppm.[52]

As the temperature is increased, the low-field NH signal shifts slightly to the higher field because of H-bond breaking. However, at 180 K, dramatic changes occur, which give rise to two broad signals at around $\delta=13.5$ and 12 ppm, whereas little changes are observed in the CH region. At 210 K, the two signals are coalesced and shifted to $\delta=11.3$ ppm. It is known from the ^{15}N NMR spectra that the proton exchange is fast, so this observation indicates the presence of a fast exchange between the NH protons and the residual OH protons of water. By integration, we obtain an intensity ratio of about 1:1:3 for the H5:H2:NH/OH atoms. At 290 K, the average NH/OH peak is further shifted to about $\delta=6.5$ ppm, and we obtain again a similar intensity ratio. This means that we have an equimolar

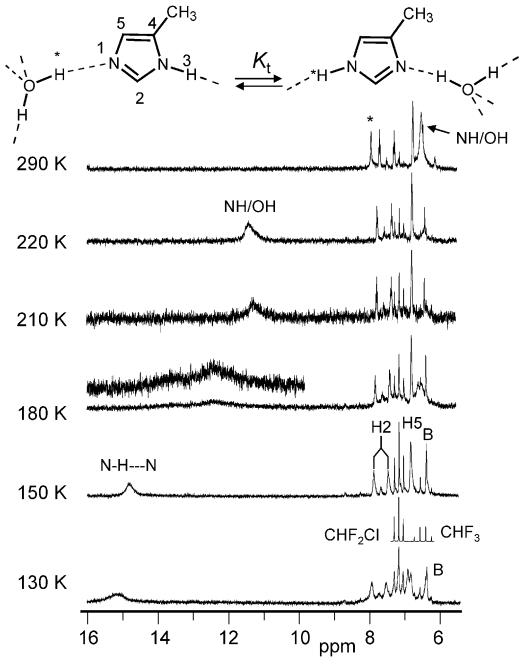

Figure 3. Variable-temperature 500.13 MHz ^{1}H NMR spectra of 4-MI-2-^{13}C,$^{15}N_2$ dissolved in wet CDF_3/CDF_2Cl, that is, of the same sample for which the ^{15}N NMR spectra were depicted in Figure 2. An unassigned impurity is labeled by an asterisk.

mixture of 4-MI and water. We also note that the H2 signal shifts slightly to the higher field when the temperature is increased, for example, to a value of $\delta=7.53$ ppm at 290 K, whereas the H5 signal remains constant.

By assuming that the chemical shift of the NH proton is similar in the NHN and the OHN hydrogen bonds and is given by $\delta_{NH}=15$ ppm, we obtain from Equation (3) values of $\delta_{H2O}=4$ ppm at 210 K and $\delta_{H2O}=2.25$ ppm at 290 K. These are typical values for fast exchange between hydrogen-bonded and non-hydrogen-bonded protons of water.[62]

$$\delta_{NH/OH}=\frac{1}{3}\delta_{NH}+\frac{2}{3}\delta_{H2O} \quad (3)$$

^{15}N CP MAS NMR spectroscopy of wild-type and mutants of human carbonic anhydrase II loaded with 4-MI-$^{15}N_2$

^{15}N CP MAS NMR experiments were performed on lyophilized solid samples of doubly ^{15}N labeled 4-MI embedded in several variants of Zn^{II} and Co^{II} HCA II.

The spectra were obtained at 240 K in order to minimize artifacts arising from an interference with molecular motions. As mentioned in the Introduction, we generally used a *z*-filter sequence in order to let the ^{15}N magnetizations equilibrate in the *z* direction of the magnetic field for 1 s. This procedure removes intensity distortions arising from cross-polarization. All of the ^{15}N chemical shifts measured are included in Table 1. The natural, abundant ^{15}N nuclei of the peptide backbone contribute an intensive peak to all spectra at around $\delta=120$–125 ppm.

The samples of Figure 4a–e were lyophilized at pH 8, at which the majority of the 4-MI molecules are neutral, because the pK_a value is 7.52.[59] Figure 4a depicts the ^{15}N NMR spectrum of the mutant H64A HCA II without addition of 4-MI-$^{15}N_2$. Only the backbone signal of the peptide amide nitrogen nuclei at natural abundance is observed at around $\delta = 124$ ppm. Figure 4b and c show the spectra obtained when 4-MI is incorporated into the wild-type enzyme. In both cases, a broad single peak is observed for the embedded 4-MI molecules at $\delta =$ 173 ppm, which is typical for imidazole nitrogen atoms exhibiting short NH distances.

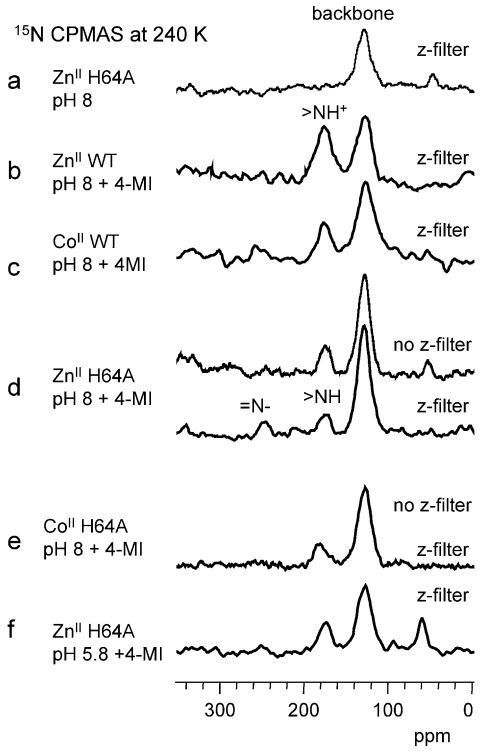

Figure 4. ^{15}N CP MAS NMR spectra (599.97 MHz for ^{1}H and 60.8 MHz for ^{15}N) of various lyophilized samples of HCA II with 4-MI-$^{15}N_2$. The spectra were obtained at 240 K. For further explanation, see the main text.

A different result was obtained for 4-MI embedded in H64A HCA II. In the absence of *z* filtering, a single amino nitrogen peak is observed at $\delta = 173$ ppm (Figure 4d). By contrast, *z* filtering leads to a signal intensity loss through spin diffusion to about half of the original value and a transfer of the lost magnetization to the adjacent nitrogen atom, with a peak appearing at $\delta = 253$ ppm. A comparison with the spectrum of bulk 4-MI-$^{15}N_2$ (Figure 2b) indicates that 4-MI is neutral and that the new low-field peak corresponds to the nonprotonated imino nitrogen atom. The longitudinal relaxation times are long and lead to a 1:1 ratio of both signals, as expected.

By contrast, in the case of the Co^{II} H64A HCA II sample (Figure 4e) only the high-field peak was observed, which lost again about half of its original signal intensity through *z* filtering, as in the case of Zn^{II} H64A HCA II. However, no signal buildup was observed for the imino nitrogen atoms.

Owing to decomposition, only a few samples were prepared at lower pH values. A spectrum of a sample of 4-MI-$^{15}N_2$ in H64A HCA II lyophilized at pH 5.8 is depicted in Figure 4f. A single peak shifted a few ppm downfield is observed, which indicates that 4-MI is now protonated. All of the results will be discussed in more detail below.

Discussion

In this discussion, we will address the following questions arising from our studies described above:

1) How can we obtain hydrogen-bond geometries and hydrogen-bond-partner information from the imidazole ^{1}H and ^{15}N chemical shifts of histidines?
2) What is the hydrogen-bonded state of 4-MI in aprotic polar solvents and of 4-MI and His64 in HCA II?
3) Are the thermodynamics and kinetics of the proton tautomerism of 4-MI influenced by water molecules?
4) Is His64 in the active site of HCA II in an aqueous or an aprotic polar environment?
5) What are the implications for the catalytic mechanism of carbonic anhydrase?

Establishing ^{1}H–^{15}N chemical-shift correlations for histidine imidazole hydrogen bonds

The question arises what the NMR chemical shifts can tell us about the protonation, hydrogen-bonding states, and hydrogen-bonding partners of the histidine imidazole rings. As has been shown by some of us for OHO,[62] OHN,[46,47,63] and NHN hydrogen bonds,[64–67] NMR parameters such as chemical shifts and coupling constants can indeed provide information about hydrogen-bond geometries. In particular, it was shown that ^{1}H and ^{15}N chemical shifts of OHN and NHN hydrogen bonds are correlated with each other, a circumstance that has been used to obtain information about OHN hydrogen-bond geometries in pyridoxal 5′-phosphate–protein interactions.[29–32] Such correlations do not only depend on the hydrogen-bond geometries but also on the chemical structure. In order to obtain information from the hydrogen bonds of the imidazole rings of histidines in biological molecules by NMR spectroscopy, we have, therefore, checked the literature for studies in which both the ^{1}H and the corresponding ^{15}N imidazole chemical shifts of histidines are reported for the regime of slow hydrogen-bond exchange and proton exchange with water. These data will be analyzed as follows.

Any hydrogen bond, AHB, is characterized by two distances, $r_1 = r_{AH}$ and $r_2 = r_{HB}$, which cannot be varied independently from each other according to neutron diffraction data, as proposed by Steiner.[68] This correlation is more conveniently discussed in terms of the heavy-atom coordinate, $q_2 = r_1 + r_2$, and the proton coordinate, $q_1 = {}^1/_2(r_1 - r_2)$. For a linear hydrogen bond, the q_2 parameter corresponds to the distance A···B and the q_1 parameter to the distance of the proton from the hydrogen-bond center. This means that when H is shifted from A to-

wards the hydrogen-bond center, the A···B distance decreases, goes to a minimum when H is located in the hydrogen-bond center, and increases again when H approaches B. This is illustrated by the geometric OHN hydrogen-bond correlation of q_2 versus q_1 (Figure 5 a), which is determined experimentally from the neutron structure and NMR data.[47] The solid line corresponds to equilibrium structures in which the volume of the proton arising from anharmonic zero-point energy motions is neglected. The dotted line represents an empirical correction for these motions. Owing to the volume of H, the shortest O···N distance cannot be realized. Therefore, the average values of q_2 around $q_1 = 0$ are located above the minimum equilibrium value of q_2. The data points in Figure 5 a stem from dipolar NMR measurements and crystallographic data reported by McDermott and co-workers.[69] They are perfectly located on the correlation curves.

It has been shown previously[47] that there is a related correlation of ^{1}H chemical shifts δ(AHN) of AHN hydrogen bonds in which A is O or N with the corresponding ^{15}N NMR chemical shifts δ(AHN), which also depends, however, on the chemical structure. As illustrated in Figure 5 b, we observe a similar correlation for histidine–imidazole hydrogen bonds, in which the ^{15}N chemical shifts are a measure for the proton coordinate q_1 and the ^{1}H chemical shifts for the heavy-atom coordinate q_2. The three curves depicted in Figure 5 b correspond to the imidazole NHN, the imidazole–carboxylic acid OHN, and the imidazole–aliphatic OHN correlation curves. They were calculated as described previously[47] by using the parameters listed in Table 3. These parameters were adapted in order to reproduce the published experimental data. The left curve limits in Figure 5 b are characterized by the limiting chemical shifts δ(N)° and δ(AH)° corresponding to free ROH (lower curve), free RCOOH (center curve), and the imino nitrogen atom of free neutral imidazole (upper curve). The right curve ends correspond to the free protonated positively charged imidazole ring and the free anion A^-, characterized by the limiting chemical shifts δ(HN)° and δ(HN)°. We note that the chemical-shift difference δ(N)°−δ(HN)° was 110 ppm, which is close to the calculated value of 120 ppm.[70]

The imidazole chemical-shift data taken from the literature and used to construct Figure 5 b are assembled in Tables S2 and S3 of the Supporting Information, including assignments and references. The data stem from various seminal studies, for example, from studies of the catalytic triad of subtilisin in aqueous solution by Bachovchin and co-workers[19,71] and by Murray and co-workers[72] or from solid-state NMR studies of histidine or the histidine side chain by the groups of McDermott,[69] Hong,[73–76] and Reif.[77,78] Blue squares are used for neutral histidine imidazole rings and red diamonds for protonated positively charged rings. These data correspond to intrinsic chemical shifts not modified by proton exchange. Unfortunately, we did not find dual ^{1}H/^{15}N data points with ^{15}N chemical shifts larger than 200 ppm, that is, molecular complexes in which the proton is located on the proton donor. We have, however, added the only data point available in this range, namely the average imino and amino chemical shifts of 4-MI in Freon obtained in this study (Figure 2, 130 K), as large circles. Clearly, they correspond to the NHN correlation curve and support the validity of the latter. We note that the NH data points of the protonated ($HisH^+$) and neutral imidazole (His) rings of histidines are located within the margin of error of about 5 ppm on the same correlation curve. This indicates

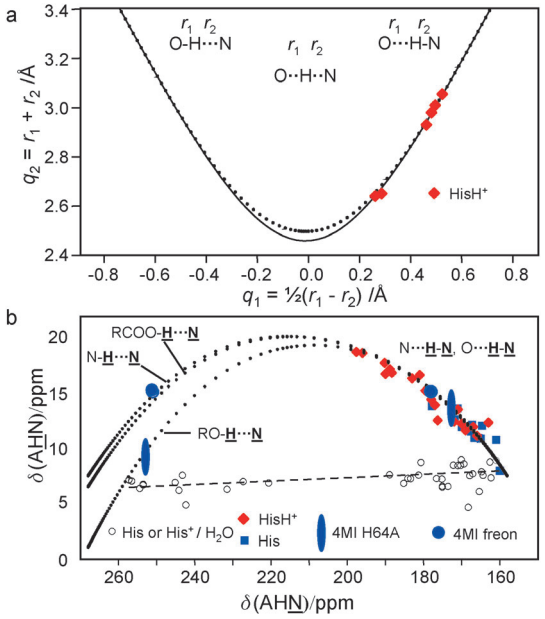

Figure 5. Hydrogen-bond correlations of imidazole rings of histidine. a) Geometric correlation of the heavy-atom coordinate $q_2 = r_1 + r_2$ as a function of the proton coordinate $q_1 = {}^1/_2(r_1 - r_2)$. For linear hydrogen bonds, q_2 represents the heavy-atom distance and q_1 the distance of the proton from the hydrogen-bond center. The solid line is valid for equilibrium structures; the dotted line represents an empirical correction for anharmonic zero-point energy vibrations, calculated as described previously.[47] The red diamonds stem from neutron diffraction and dipolar NMR data of imidazole rings published by McDermott and co-workers.[69] b) ^{1}H versus ^{15}N chemical-shift correlation of hydrogen-bonded imidazole rings of histidines. The data plotted are assembled in Table S2 in the Supporting Information. The large blue circles stem from 4-MI in Freon at 130 K (Figure 2). The vertical blue ellipsoids represent the data of 4-MI in the H64A mutant of HCA II. For further explanation, see the text.

Table 3. Parameters of the ^{1}H–^{15}N NMR chemical-shift correlations of the imidazole rings of histidines.[a]

Limiting imidazole ^{15}N chemical shift of the imino nitrogen atom	δ(N)°	268
Limiting imidazole ^{15}N chemical shift of the amino nitrogen atom	δ(HN)°	158
Limiting imidazole ^{1}H chemical shift of the amino nitrogen atom	δ(HN)°	7.5
Excess ^{1}H chemical shift of the strongest NHN hydrogen bond	Δ(NHN)	15
Excess ^{15}N chemical shift of the strongest OHN and NHN hydrogen bonds	Δ(AHN)	0
Limiting ^{1}H chemical shift of free RCOOH	δ(OH)°	6
Excess ^{1}H chemical shift of the strongest RCOOHN hydrogen bond	Δ(OHN)	15
Limiting ^{1}H chemical shift of free ROH	δ(OH)°	1
Excess ^{1}H chemical shift of the strongest ROHN hydrogen bond	Δ(OHN)	17

[a] Chemical shifts, δ, are given in ppm. For definitions of the symbols, see the text and reference [47].

that the small low-field ^{15}N shift of $HisH^+$ relative to His observed frequently (Table S2 in the Supporting Information) is also correlated to a small ^1H low-field shift, that is, with slightly stronger hydrogen bonds after protonation. Moreover, the differences in the ^{15}N chemical shifts of the two nitrogen atoms are also in the order of the margin of error. Finally, for later discussion, we have included in Figure 5b the ^{15}N chemical shifts of 4-MI in H64A HCA II lyophilized at pH 7.8 as vertical elongated ellipses, because we do not know the corresponding ^1H chemical shifts.

In order to demonstrate the effect of exchange with water, we include in Figure 5b for comparison one set of histidine data (open circles) reported by Wolff et al.[79] for an aqueous solution of gallium–protoporphyrin IX in the hemophore HasASM. Thus, a ^1H chemical shift below 8 ppm and a ^{15}N chemical shift between 170 and 250 ppm indicate that the tautomerism of the imidazole ring is coupled to a fast proton exchange with water.

In order to estimate distances from $^1H/^{15}N$ chemical shifts more easily than with the calculation procedure described previously,[47] we compare in Figure 6 correlations of the ^1H chemical shifts with the q_1 parameter and of the r_1 and r_2 values with the ^{15}N chemical shifts, calculated by using empirical Equations (4) and Equation (5), which have to be used with the parameters listed in Table 3.

$$r_2 = r_{HN} = 0.992 - 0.385 \times \ln\frac{\delta(\underline{N})^\circ - \delta(OH\underline{N})}{\delta(\underline{N})^\circ - \delta(H\underline{N})^\circ} \quad (4a)$$

$$r_1 = r_{OH} = 0.942 - 0.371 \times \ln[1 - \exp\{(0.992 - r_2)/0.385\}] \quad (4b)$$

$$\delta(OH\underline{N}) = 0.5(\delta(O\underline{H})^\circ + \delta(H\underline{N})^\circ) + 0.5(\delta(O\underline{H})^\circ - \delta(H\underline{N})^\circ) \times \left(\frac{1 - \exp(q_1/0.385)}{1 + \exp(q_1/0.385)}\right) + 13.1\exp(-5.2(q_1 + 0.0003)^2) \quad (5)$$

It is beyond the scope of this study to estimate hydrogen-bond geometries of all of the data points in Figure 5b and the corresponding hydrogen-bond distances. We only want to highlight the largest ^1H chemical shifts of about 19 ppm associated with a ^{15}N chemical shift of 200 ppm reported by Halkides et al.[72] and by Lopez del Amo et al.[78] By assuming linear hydrogen bonds, we estimate a very short N···O distance of about 2.53 Å and O···H and H···N distances of 1.35 and 1.18 Å, by using Figures 5 and 6 and/or [Eqs. (5) and (4)].

In conclusion, the histidine imidazole ^1H–^{15}N chemical-shift correlation of Figures 5b and 6 allows one to decide whether NH proton exchange with water takes place and to estimate hydrogen-bond geometries. The correlations proposed are preliminary, because the body of experimental data does not yet cover the whole chemical-shift range. Therefore, the correlations can only give semiquantitative results at present. However, it may be a guideline for a search of ^1H chemical shifts of O–H···N hydrogen bonds of histidine imidazole rings to provide information about the hydrogen-bond partner.

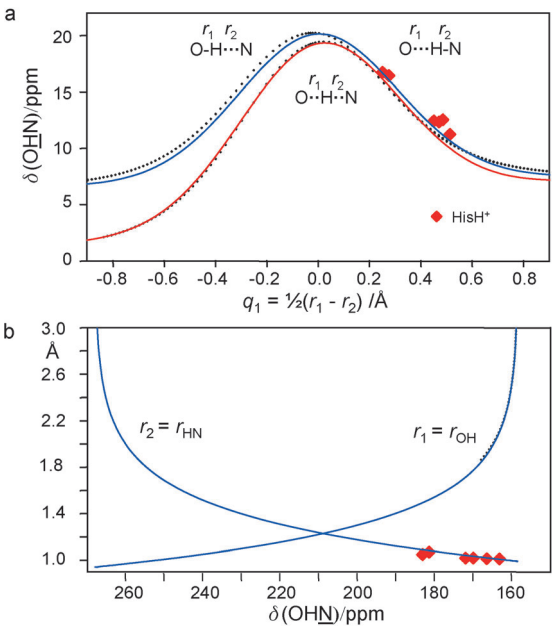

Figure 6. a) ^1H chemical shifts $\delta(O\underline{H}N)$ of imidazole rings as a function of the proton coordinate $q_1 = {}^1/_2(r_1 - r_2)$. The dotted line was calculated as described previously;[47a] the solid line was calculated by using Equation (4). b) The O···H distance r_1 and the H···N distance r_2 as a function of the ^{15}N chemical shift $\delta(OH\underline{N})$ calculated by using Equation (5). The red diamonds stem from the neutron diffraction and dipolar NMR data of imidazole rings published by McDermott and co-workers.[69] For further explanation, see the main text.

Proton exchange mechanism and hydrogen-bond association of 4-MI in Freon

For the later discussion, we need to discuss these topics in more detail. As depicted in Figure 2, we found slow proton exchange at 130 K but fast proton exchange already at 210 K. A very rough estimate yields inverse lifetimes of about 300 s^{-1} at 130 K and of 10^5 s^{-1} at 210 K, from which we estimate an energy of activation of about 20 kJ mol^{-1} and a frequency factor of 10^{11} s^{-1}. That would lead to an inverse lifetime of about 10^7 s^{-1} at 298 K. We note that this exchange is much faster than the proton exchange within cyclic dimers, trimers, and tetramers of pyrazole molecules in the solid state.[80]

The ^1H spectra of 4-MI in Freon (Figure 3) indicate that the tautomerism observed by ^{15}N NMR spectroscopy is coupled to the exchange of the NH protons with the OH protons of water. Without water, the proton exchange is slow. Above 200 K, only averaged NH/OH signals are observed. Signal integration indicates a 2:1 4-MI/H_2O ratio at 210 K and 220 K but a 1:1 ratio at 290 K. Water precipitates as ice at low temperatures, and we think that it has more or less left the solution at 130 K, although single water molecules could remain hydrogen bonded between two 4-MI molecules, as in the case of 2,4,6-trimethylpyridine (collidine)–water mixtures in Freon.[36] This means that we have a majority of NHN hydrogen bonds at 130 K but mostly OHN hydrogen bonds at 210 K and above.

However, whereas proton exchange becomes fast only at around 210 K, the interconversion of different hydrogen-bonded species is fast in the whole temperature range. For 130 K, we have to discuss several rapidly interconverting hy-

drogen-bond associates, as depicted in Scheme 3 and Scheme 4. For simplification, substituents such as methyl groups are omitted. Firstly, one needs to consider hydrogen-bonded chains of different length (Scheme 3a), most probably disordered with respect to the two tautomers, as observed for the undercooled melt of 4-MI by Zimmermann in 1958.[43] For the gas phase, computations by Poterya et al.[81] have shown that, besides cyclic trimers, the most stable imidazole cluster is the cyclic tetramer depicted in Scheme 3b. Similar clusters could be formed in Freon, but some hydrogen bonds will be broken upon temperature increase, for example, to 150 K, as illustrated in Scheme 3c–f, which can explain the observed high-field shift of the NH proton signal (Figure 3).

On the other hand, when the temperature is increased, the free amino and imino groups of 4-MI may become available as proton donors and acceptors. Miller and co-workers[82] have observed experimentally monomers, linear dimers, and linear trimers of imidazole in helium droplets at 20 K hydrogen bonded to one water molecule, both as donors and as acceptors (Scheme 4a). Jagoda-Cwiklik et al.[83] have calculated the structures of a single imidazole with one or more water molecules, as depicted schematically in Scheme 4b. The 1:4 cluster exhibits a cyclic structure in which a degenerate quadruple proton transfer could occur. Such complexes could also be present in Freon. They might also form first an open and then a cyclic structure (Scheme 4c), in which protons might be exchanged. However, the proton exchange might be more complex, for example, coupled to hydrogen-bond switches of NH and OH groups. The establishment of further information about the proton and hydrogen-bond exchange of 4-MI was, however, beyond the scope of this study. Later, we will, however, come back to the problem of how the equilibrium constant of tautomerism of 4-MI in Freon is influenced by the presence of water.

Protonation state (pK_a) and hydrogen-bond state of 4-MI in Zn^{II} H64A HCA II and Co^{II} H64A HCA II

Let us now discuss the solid-state ^{15}N NMR spectra of 4-MI-$^{15}N_2$ in different lyophilized carbonic anhydrases (Figure 4). We employed *z* filtering, which allows the ^{15}N magnetization to equilibrate after cross-polarization in the *z* direction. Thus, the imino and the amino nitrogen signals of neutral 4-MI, the tautomerism of which is quenched, will both appear in the spectrum as long as the spin diffusion rates are larger than the longitudinal relaxation rates, a condition usually fulfilled for organic solids.[53]

When we embedded 4-MI-$^{15}N_2$ in wild-type Zn^{II} and Co^{II} HCA II, we observed only a single line that is typical for protonated 4-MI (Figure 4b and c), with a ^{15}N chemical shift of $\delta =$ 173 ppm (Table 1). The correlation of Figure 5b indicates that such a value corresponds to a medium to strong hydrogen bond. The active site is blocked by His64, so we assign this signal to 4-MI bound to other residues of the enzyme. We tentatively assign this signal to an OHN hydrogen bond or salt bridge between an aspartate or glutamate residue and protonated 4-MI. As discussed previously, when carboxylate and a neutral heterocyclic imino nitrogen come close to each other somewhat away from the water phase, their basicity increases and they catch a proton from the aqueous phase.[29] Another possibility is the occurrence of cooperative interactions between several proton donors, which can dramatically increase the proton-donating ability of one of these groups and protonate 4-MI.[84] In principle, one might also discuss the binding of 4-MI to sites 2–8, reported by Aggarwal et al.[15] for 4-MI in H64A HCA II, in which each site corresponds to a cavity formed by several amino acid residues. However, these sites were observed when H64A HCA II and 4-MI were cocrystallized at a ratio of 1:300, whereas 1:1 ratios were always employed in the samples used to generate Figure 4.

By contrast, Aggarwal et al.[15] had also shown that 4-MI in H64A HCA II is located almost in the same positions as His64 in the wild-type enzyme. This is

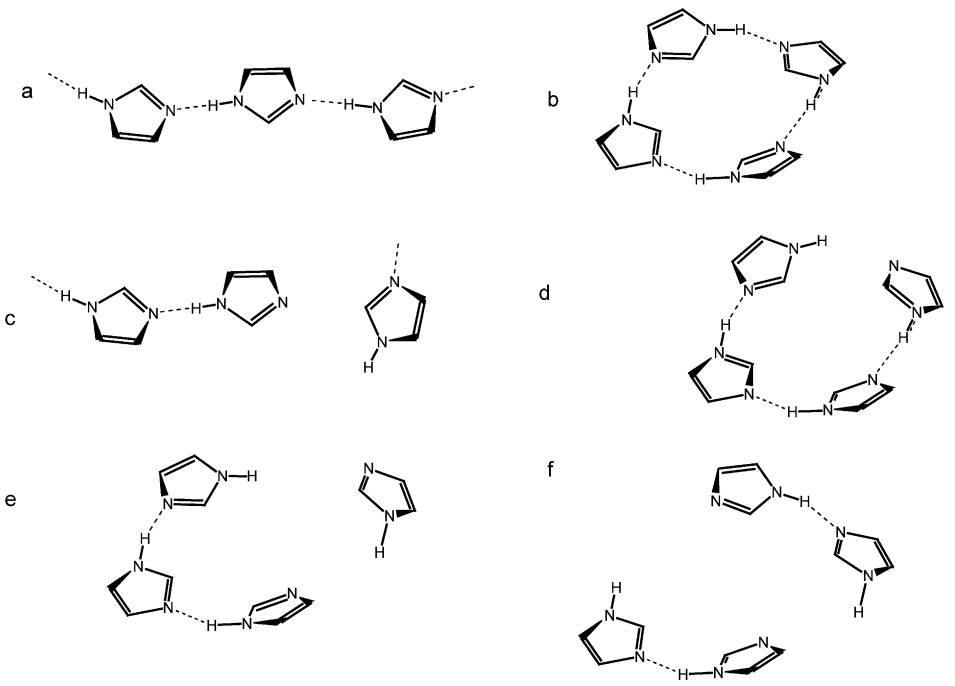

Scheme 3. Potential hydrogen-bonded clusters of 4-MI in Freon in the absence of water. a) Hydrogen-bonded chains of 4-MI molecules according to Zimmermann.[43] b) Formation of cyclic hydrogen-bonded tetramers of imidazole in the gas phase in accordance with the calculations of Poterya et al.[81] c) Hydrogen-bond opening of a chain of 4-MI molecules in the liquid state upon an increase in temperature. d)–f) Corresponding opening process of cyclic tetramers. For simplification, methyl groups and other substituents are omitted.

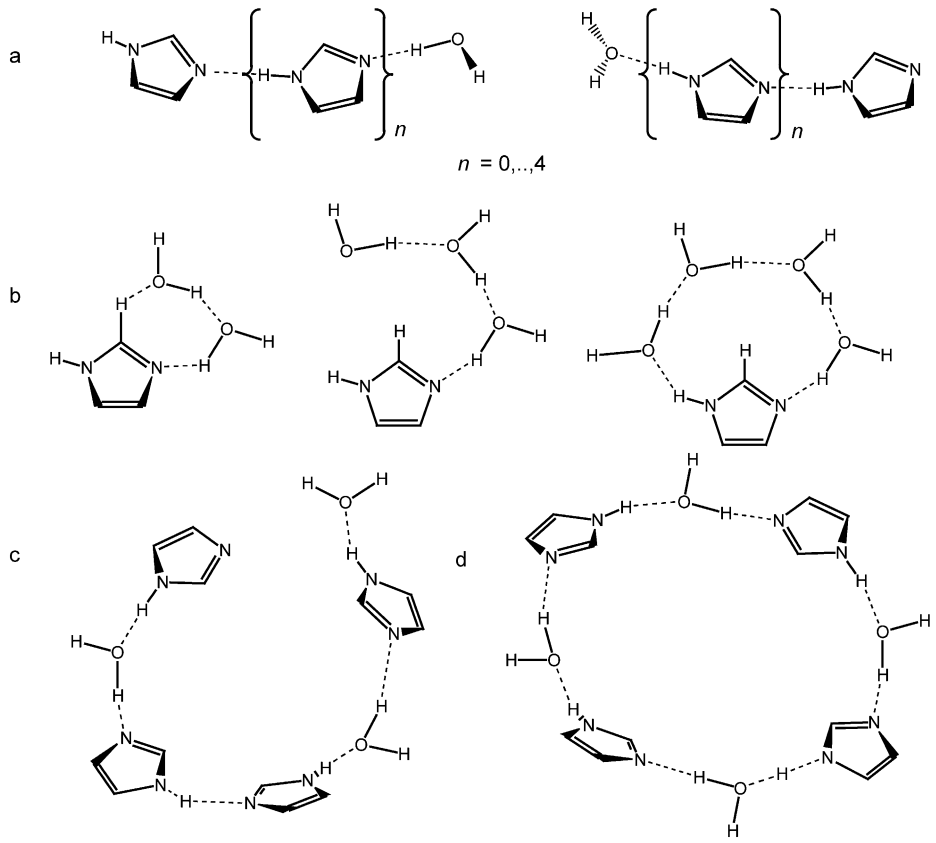

Scheme 4. Schematic structure of potential hydrogen-bonded clusters of 4-MI in Freon in the presence of water. a) Imidazole–water clusters observed by vibrational spectroscopy in helium droplets at 20 K according to Miller and co-workers.[82] b) Imidazole–water clusters calculated by Jagoda-Cwiklik et al.[83] c) Open 4:3 cluster. d) Regular cyclic 4:4 cluster.

consistent with our findings: in contrast to the ^{15}N NMR spectrum of 4-MI in the wild-type enzyme, after lyophilization at around pH 8, 4-MI binds as a neutral molecule to H64A HCA II, as indicated by the observation of a signal at $\delta = 173$ ppm for the amino group and at $\delta = 253$ ppm for the imino group (Figure 4e). The latter signal was observed only after magnetization transfer through spin diffusion for 1 s from the amino to the imino nitrogen atoms. 4-MI is protonated in all other binding sites, so it must have been loaded into the active-site cavity of H64A HCA II. We propose a binding in the inward conformation, in agreement with the calculations of Maupin et al.[10,22] Lyophilization at pH 5.8 leads to protonated 4-MI in H64A HCA II (Figure 4g). In this case, 4-MI-H^+ might not stay in the active site but might switch at least to the outward position, as suggested by Maupin et al.[10,22] In other words, as soon as 4-MI receives a proton from zinc-bound water, 4-MI moves out of the active-site cavity. This implies a major change of the pK_a value inside the cavity relative to aqueous solution. Note, however, that the term "pK_a value" is not well defined in the interior of a protein, as has been discussed recently.[85]

We made further attempts to localize 4-MI in H64A HCA II by substituting the Zn ion for a paramagnetic Co ion. Previously, Elder et al.[16] had measured and analyzed the ^1H relaxivity of 4-MI induced by the paramagnetic Co^{II} ion in aqueous Co^{II} H64A HCA II solutions. By using these data, the proximity of 4-MI to the Co^{II} ion was established and the binding constants of 4-MI were measured. According to these results, under the conditions and pH 8 in which our samples were prepared, all 4-MI was bound in the active site.

In contrast to the liquid state, the molecular motions are strongly reduced in solid samples, and we did not expect to probe the proximity of 4-MI to the paramagnetic Co^{II} ion through relaxometry. By contrast, we hoped to detect pseudocontact shifts (pcs) of the nitrogen atoms of 4-MI-$^{15}N_2$ caused by the proximity of the paramagnetic Co^{II} ion.

However, when we measured the ^{15}N NMR spectra of 4-MI-$^{15}N_2$ in Co^{II} H64A HCA II lyophilized at pH 8 (Figure 4e), we observed only a single line at around $\delta =$ 180 ppm. As compared with the results with Zn^{II} H64A HCA II, this indicates a small low-field shift. As in the Zn^{II} H64A HCA II case, the signal lost about half of its intensity by *z* filtering, as illustrated in Figure 4e.

There are two hypotheses to explain the observation of the single peak for Co^{II} H64A HCA II:

Hypothesis 1: One could argue that 4-MI is protonated, although the sample was lyophilized at pH 8, and not loaded into the active site near the Co^{II} ion. This would, however, represent an unprecedented major chemical difference of acid–base behavior between Co^{II} H64A HCA II and Zn^{II} H64A HCA II, which seems to be unlikely because both enzymes catalyze the hydration of CO_2 in a similar way.[16]

Hypothesis 2: One could assume that 4-MI is neutral and placed, as in the case of Zn^{II} H64A HCA II, in the active site of Co^{II} H64A HCA II. This would explain the loss of magnetization by *z* filtering. The small low-field shift of the amino signal could then, at least to some extent, represent a pcs. The absence of the imino signal may then arise from a larger pcs or from line broadening arising from various magnetic interactions with the paramagnetic Co^{II} ion.

In this context, we note that Banci et al.[86] have performed ^1H NMR experiments on Zn^{II}- and Co^{II}-substituted bovine carbonic anhydrase. For protons of Co ligands, the pcs varied between -100 ppm and $+50$ ppm, whereas values between -50 ppm and $+18$ ppm were found for nonligand protons. Interestingly, the H2 atom of His64 exhibited a pcs of only a few

ppm. Thus, one could also expect very different values for the imino and amino nitrogen signals of 4-MI in Co^{II} H64A HCA II. This second explanation does not contain contradictions at present; therefore, we think that hypothesis 2 is more likely than hypothesis 1.

Histidine imidazole H-bond geometries of HCA II

What can we tell about the state of 4-MI in H64A HCA II? Unfortunately, we were not able to tell which of the two tautomers in Scheme 2 was formed. We estimate that their mole fractions are similar. Thus, the imino nitrogen (=N–) signal could stem from the N1 atom in the π tautomer and/or from the N3 atom in the τ tautomer (see Scheme 2). Similarly, the origin of the amino nitrogen (>NH) signal could be either the N3H group in the π tautomer and/or the N1H group in the τ tautomer.

However, we can say that both nitrogen atoms of 4-MI form hydrogen bonds, and the hydrogen-bond partner must be oxygen, most probably from water. Thus, the imino nitrogen atoms of 4-MI form O–H···N and the amino nitrogen atoms form O···H–N hydrogen bonds. By using [Eq. (4)] and assuming linear hydrogen bonds, we estimate an O···H distance of 1.05 Å and an H···N distance of 1.76 Å for the imino O–H···N hydrogen bond, that is, an O···N distance of 2.81 Å. For the amino nitrogen atom, an O···H–N hydrogen bond, we estimate an O···H distance of 1.73 Å and an H···N distance of 1.05 Å, that is, an O···N distance of about 2.78 Å.

Are these results also representative for His64 in the wild-type enzyme? We note that the arithmetic mean of the imino and amino ^{15}N chemical shifts of 4-MI-$^{15}N_2$ in H64A HCA II is 213 ppm. This value is close to the value of 208 ppm reported for the two nitrogen atoms of His64 in HCA II at pH 8, in which the imidazole ring is neutral and exhibits a fast degenerate proton exchange, most probably with water molecules.[20] This indicates a similar state of His64 in the wild-type enzyme and of 4-MI in the mutant, although this value is not very specific.

On the other hand, the shortest distance of a His64 nitrogen atom in HCA II to the nearest ordered water oxygen atom was found to be 3.5 Å (Figure 1).[9] However, disordered water molecules are not observed by X-ray crystallography, and it could be that the active-site water molecules in H64A HCA II are disordered in the lyophilized solid mutant in such a way that the O···N distances are shorter and allow for hydrogen-bond formation.

The equilibrium constant of the tautomerism of monosubstituted imidazoles: a sensor for the local environment

Let us now address the question of whether our NMR experiments of 4-MI in the polar but aprotic Freon can help us to understand the state and function of His64 in HCA II. We showed that not only the kinetics of the proton tautomerism of 4-MI is influenced by the presence of water molecules but also the equilibrium constant of tautomerism, K_t, for 4-MI increases upon hydration, which leads to a preference for the τ tautomer (Scheme 2). Whereas the K_t value is unity in the absence of water in solutions of 4-MI in the polar aprotic Freon, it increases to 1.09 at 290 K when the number of water molecules and of 4-MI are the same. By contrast, for 4-MI in water at pH 11, a value of $K_t = 1.5$ has been reported.[61] We observed in this study at pH 12 a value of 1.58, which is in excellent agreement. This trend, that hydrogen bonds of 4-MI to water molecules increase the K_t value, has been confirmed in quantum-mechanical calculations of Luque et al.,[87] Li et al.,[88] and Nagy et al.[89]

This value is much smaller than the values for the neutral imidazole ring of histidine reported by Blomberg et al.[17] or of neutral histidine residues at the protein surface of HCA II, as shown by Shimahara et al.[20] The finding of the latter authors of a value of $K_t = 1$ for the imidazole ring of His64 in the active site is an important indication that the active-site environment does not resemble the one in aqueous solution but more the aprotic polar Freon environment that contains only a small number of water molecules.

Mechanism of tautomerism of the imidazole ring of His64 in HCA II

What could be the mechanism of tautomerism of the imidazole ring of His64 in the inward position of the active site of HCA II? By combining the X-ray crystal structure of HCA II (Figure 1) with those proposed in Scheme 4 for 4-MI in wet Freon, we arrive at the scenario depicted in Scheme 5. We estimated the rate of proton exchange in Freon, that is, of the interconversion of the two tautomers, to be at least about $10^7\ s^{-1}$ at 298 K. That value implies very fast reorientation of the imidazole ring and fast rearrangement of the hydrogen-bonded imidazole–water network. The properties of the non-aqueous environment in the active site of HCA II will be similar and will allow fast reorientation of the imidazole ring of His64 and rearrangement of the hydrogen-bond network. Maupin et al.[10,22] computed an energy barrier of 5.6–6.2 kcal mol^{-1} for the interconversion of inward and outward orientations. This is considerably less than the energy barrier for proton transfer in catalysis, which is near 10 kcal mol^{-1}. Thus, it is conceivable that the initial state derived from the X-ray crystal structure can rapidly form a cyclic imidazole–$(H_2O)_4$ complex, in which the π to τ tautomerism takes place through a concerted or stepwise multiple proton transfer.

Implication for the biological function

Let us now discuss the implications of the above findings for the role and function of His64 in HCA II. In Figure 7, the different states discussed above in Scheme 1 are depicted schematically. Above pH 7.2, the imidazole ring is neutral and forms state **1**, in which it is subjected to a fast degenerate tautomerism with $K_t = 1$,[20] associated with a fast rearrangement of the hydrogen bonds of water and the imidazole. This situation resembles the one found herein for 4-MI in wet Freon at room temperature. Thus, the environment of His64 in the inward conformation exhibits a lower dielectric constant than that in the aqueous phase, as illustrated by the different colors. If the neutral imidazole ring were immersed in the outward position

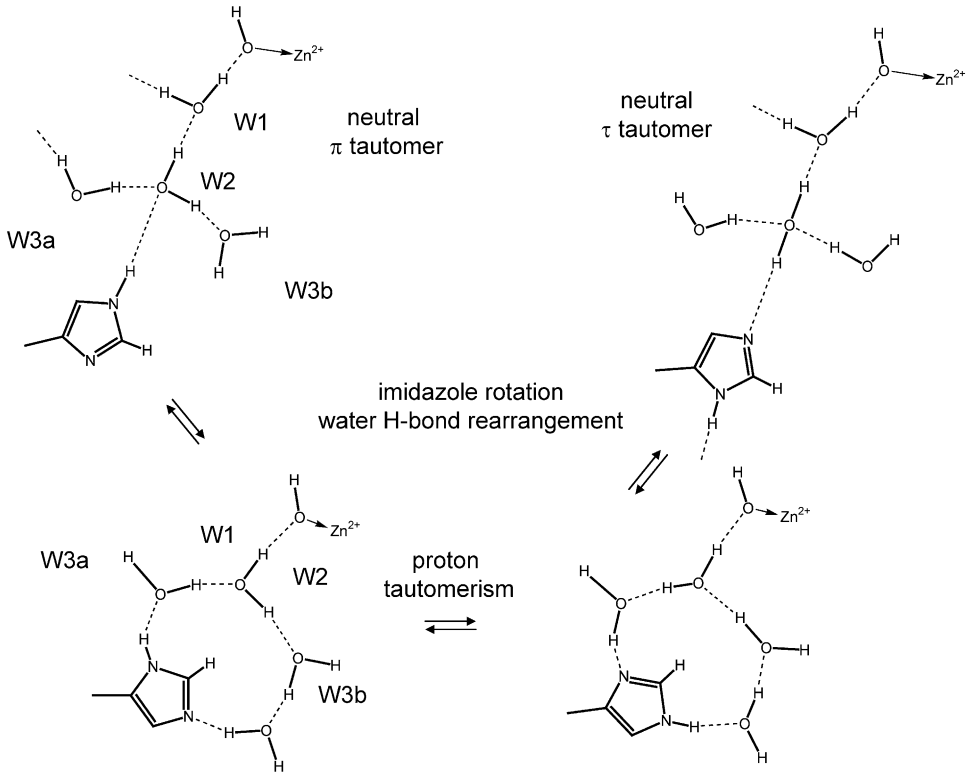

Scheme 5. Scenario of proton tautomerism of the imidazole ring of His64 in the active site of HCA II derived from the crystal structure (Figure 1) and the clusters depicted in Scheme 4. For further explanation, see the main text.

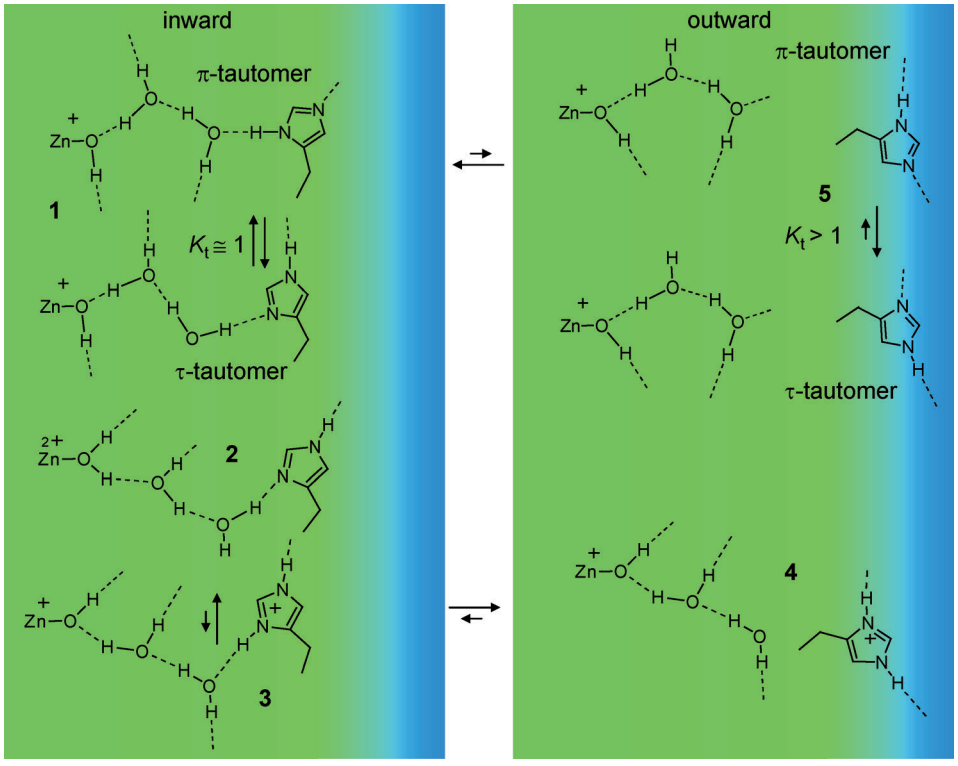

Figure 7. Environment-dependent tautomerism and protonation/deprotonation of the imidazole ring of His64 in HCA II. The blue color indicates that the aqueous phase is polar, whereas the active-site environment is less polar. The observation that, at pH > 7.2, the neutral imidazole ring exhibits an equilibrium constant of $K_t \cong 1$,[20] means that it is located in the inward conformation, that is, in the less polar environment. In the polar aqueous phase $K_t > 1$. When the imidazole ring is protonated, it prefers the outward conformation, in which it rapidly loses the proton and comes back to the inward conformation.

in the aqueous phase (state **5**), the equilibrium constant would be larger than unity. Thus, as long as the imidazole ring is neutral, it must be located in the inward position (state **1**). This finding is in agreement with the calculations of Maupin et al.[22]

The situation will be different when water is coordinated to the Zn^{II} ion (state **2** in Scheme 1 and Figure 7). The calculations of Maupin et al.[10] showed for this situation that proton transfer to imidazole (state **3**) constitutes an uphill process that leads to an immediate conformational change to the outward position (state **4**), in which the proton is transferred to the buffer to form state **5**. That state will, however, immediately reconvert to state **1** above pH 7.2. By contrast, at lower pH values, state **2** will be preferred.

Conclusion

The main conclusions of the present study can be summarized as follows.

1) ^{1}H and ^{15}N chemical shifts of imidazole rings of histidines are correlated, from which information on the hydrogen-bond geometries and on the tautomerism can be derived. We anticipate that the correlation might be useful to understand other proteins, for example, histidines in transmembrane proton channels.[74–76]
2) NMR studies of ^{15}N-labeled 4-methylimidazole (4-MI) in the polar solvent CDF_3/CDF_2Cl down to 130 K reveal that the π to τ tautomerism is degenerate in aprotic polar medium, whereas the addition of water favors the τ tautomer. Water molecules also catalyze the tautomerism.
3) 4-MI represents a local NMR probe, which was incorporat-

ed into the mutant H64A of human carbonic anhydrase II (HCA II), in which the active-site histidine was replaced by alanine, and the catalytic activity was rescued by 4-MI.

4) The finding of a degenerate tautomerism of His64 HCA II indicates that its imidazole ring is located in the inward position and that the active-site environment resembles the one of wet polar organic solvents rather than an aqueous environment. However, it would be desirable in the future to perform diffusion or NOE experiments on 4-MI in isotopically labeled H64A HCA II in order to obtain more information about the binding sites, which would enable a comparison with the crystallographically determined sites.[15]
5) The results support the view that protonation of the imidazole ring of His64 leads to a switch of the ring to the outward conformation, in which the proton is delivered to the aqueous phase. This is consistent with the first observation of the change in His64 conformations, as observed previously.[11]
6) Many open questions remain that concern details of the above-mentioned processes, and further experimental and theoretical studies may be required.

Acknowledgements

We thank the Deutsche Forschungsgemeinschaft, Bonn (Li300/25-1) and the Russian Foundation of Basic Research (Projects 14-03-00111 and 14-03-00716) for financial support.

Keywords: enzyme catalysis · enzyme models · hydrogen bonds · NMR spectroscopy · tautomerism

[1] a) H. Steiner, B. H. Jonsson, S. Lindskog, *Eur. J. Biochem.* **1975**, *59*, 253 – 259; b) S. Lindskog, *Pharmacol. Ther.* **1997**, *74*, 1 – 20.
[2] D. W. Christianson, C. A. Fierke, *Acc. Chem. Res.* **1996**, *29*, 331 – 339.
[3] D. N. Silverman, R. McKenna, *Acc. Chem. Res.* **2007**, *40*, 669 – 675.
[4] C. T. Supuran, A. Scozzafava, *Expert Opin. Ther. Pat.* **2000**, *10*, 575 – 600.
[5] R. L. Mikulski, D. N. Silverman, *Biochem. Biophys. Acta Proteins Proteomics* **2010**, *1804*, 422 – 426.
[6] S. Z. Fisher, A. Y. Kovalevsky, J. F. Domsic, M. Mustyakimov, R. McKenna, D. N. Silverman, P. A. Langan, *Biochemistry* **2010**, *49*, 415 – 421.
[7] D. N. Silverman, C. Tu, X. Chen, S. M. Tanhauser, A. J. Kresge, P. J. Laipis, *Biochemistry* **1993**, *32*, 10757 – 10762.
[8] S. Z. Fisher, C. M. Maupin, M. Budayova-Spano, L. Govindasamy, C. Tu, M. Agbandje-McKenna, D. N. Silverman, G. A. Voth, R. McKenna, *Biochemistry* **2007**, *46*, 2930 – 2937.
[9] B. S. Avvaru, C. U. Kim, K. H. Sippel, S. M. Gruner, M. Agbandje-McKenna, D. N. Silverman, R. McKenna, *Biochemistry* **2010**, *49*, 249 – 251.
[10] a) C. M. Maupin, R. McKenna, D. N. Silverman, G. A. Voth, *J. Am. Chem. Soc.* **2009**, *131*, 7598 – 7608; b) C. M. Maupin, J. Zheng, C. Tu, R. McKenna, D. N. Silverman, G. A. Voth, *Biochemistry* **2009**, *48*, 7996 – 8005.
[11] S. K. Nair, D. W. Christianson, *J. Am. Chem. Soc.* **1991**, *113*, 9455 – 9458.
[12] a) H. An, C. Tu, D. Duda, I. Montanez-Clemente, K. Math, P. J. Laipis, R. McKenna, D. N. Silverman, *Biochemistry* **2002**, *41*, 3235 – 3242; b) D. Duda, C. Tu, M. Qian, P. Laipis, M. Agbandje-McKenna, D. N. Silverman, R. McKenna, *Biochemistry* **2001**, *40*, 1741 – 1748.
[13] C. Tu, D. N. Silverman, C. Forsman, B. H. Jonsson, S. Lindskog, *Biochemistry* **1989**, *28*, 7913 – 7918.
[14] D. Duda, L. Govindasamy, M. Agbandje-McKenna, C. Tu, D. N. Silverman, R. McKenna, *Acta. Crystallogr. Sect. D* **2003**, *59*, 93 – 104.
[15] M. Aggarwal, B. Kondeti, C. Tu, C. M. Maupin, D. N. Silverman, R. McKenna, *IUCrJ* **2014**, *1*, 129 – 135.
[16] I. Elder, C. Tu, L. J. Ming, R. McKenna, D. N. Silverman, *Arch. Biochem. Biophys.* **2005**, *437*, 106 – 114.
[17] F. Blomberg, W. Maurer, H. Rüterjans, *J. Am. Chem. Soc.* **1977**, *99*, 8149 – 8159.
[18] N. Shimba, H. Takahashi, M. Sakakura, I. Fuji, I. Shimada, *J. Am. Chem. Soc.* **1998**, *120*, 10988 – 10989.
[19] R. M. Day, C. J. Thalhauser, J. L. Sudmeier, M. P. Vincent, E. V. Torchilin, D. G. Sanford, C. W. Bachovchin, W. W. Bachovchin, *Protein Sci.* **2003**, *12*, 794 – 810.
[20] H. Shimahara, T. Yoshida, Y. Shibata, M. Shimizu, Y. Kyogoku, F. Sakiyama, T. Nakazawa, S. Tate, S. Ohki, T. Kato, H. Moriyama, K. Kishida, Y. Tano, T. Ohkubo, Y. Kobayashi, *J. Biol. Chem.* **2007**, *282*, 9646 – 9656.
[21] I. D. Campbell, S. Lindskog, A. I. White, *J. Mol. Biol.* **1975**, *98*, 597 – 614.
[22] C. M. Maupin, G. A. Voth, *Biochemistry* **2007**, *46*, 2938 – 2947.
[23] S. Toba, G. Colombo, K. M. Merz, *J. Am. Chem. Soc.* **1999**, *121*, 2290 – 2302.
[24] M. Elstner, Q. Cui, P. Munih, E. Kaxiras, T. Frauenheim, M. Karplus, *J. Comput. Chem.* **2003**, *24*, 565 – 579.
[25] Z. Smedarchina, W. Siebrand, A. Fernández-Ramos, Q. Cui, *J. Am. Chem. Soc.* **2003**, *125*, 243 – 251.
[26] C. M. Schutz, A. Warshel, *J. Phys. Chem. B* **2004**, *108*, 2066 – 2075.
[27] S. Braun-Sand, M. Strajbl, A. Warshel, *Biophys. J.* **2004**, *87*, 2221 – 2239.
[28] S. B. Lesnichin, I. G. Shenderovich, T. Muljati, D. N. Silverman, H. H. Limbach, *J. Am. Chem. Soc.* **2011**, *133*, 11331 – 11338.
[29] a) S. Sharif, E. Fogle, M. D. Toney, G. S. Denisov, I. G. Shenderovich, P. M. Tolstoy, M. Chan-Huot, G. Buntkowsky, H. H. Limbach, *J. Am. Chem. Soc.* **2007**, *129*, 9558 – 9559; b) M. Chan-Huot, A. Dos, R. Zander, S. Sharif, P. M. Tolstoy, S. Compton, E. Fogle, M. D. Toney, I. G. Shenderovich, G. S. Denisov, H. H. Limbach, *J. Am. Chem. Soc.* **2013**, *135*, 18160 – 18175.
[30] S. Sharif, D. Schagen, M. D. Toney, H. H. Limbach, *J. Am. Chem. Soc.* **2007**, *129*, 4440 – 4455.
[31] S. Sharif, G. S. Denisov, M. D. Toney, H. H. Limbach, *J. Am. Chem. Soc.* **2006**, *128*, 3375 – 3387.
[32] S. Sharif, G. S. Denisov, M. D. Toney, H. H. Limbach, *J. Am. Chem. Soc.* **2007**, *129*, 6313 – 6327.
[33] N. S. Golubev, I. G. Shenderovich, S. N. Smirnov, G. S. Denisov, H. H. Limbach, *Chem. Eur. J.* **1999**, *5*, 492 – 497.
[34] I. G. Shenderovich, P. M. Tolstoy, N. S. Golubev, S. N. Smirnov, G. S. Denisov, H. H. Limbach, *J. Am. Chem. Soc.* **2003**, *125*, 11710 – 11720.
[35] S. B. Lesnichin, P. M. Tolstoy, H. H. Limbach, I. G. Shenderovich, *Phys. Chem. Chem. Phys.* **2010**, *12*, 10373 – 10379.
[36] S. Sharif, I. G. Shenderovich, L. Gonzalez, G. S. Denisov, D. N. Silverman, H. H. Limbach, *J. Phys. Chem. A* **2007**, *111*, 6084 – 6093.
[37] S. Kong, A. O. Borissova, S. B. Lesnichin, M. Hartl, L. L. Daemen, J. Eckert, M. Yu. Antipin, I. G. Shenderovich, *J. Phys. Chem. A* **2011**, *115*, 8041 – 8048.
[38] B. Wehrle, H. Zimmermann, H. H. Limbach, *J. Am. Chem. Soc.* **1988**, *110*, 7014 – 7024.
[39] D. Mauder, D. Akcakayiran, S. B. Lesnichin, G. H. Findenegg, I. G. Shenderovich, *J. Phys. Chem. C* **2009**, *113*, 19185 – 19192.
[40] A. A. Gurinov, D. Mauder, D. Akcakayiran, G. H. Findenegg, I. G. Shenderovich, *ChemPhysChem* **2012**, *13*, 2282 – 2285.
[41] I. Fischbach, H. W. Spiess, K. Saalwächter, G. R. Goward, *J. Phys. Chem. B* **2004**, *108*, 18500 – 18508.
[42] B. S. Hickman, M. Mascal, J. Titman, I. G. Wood, *J. Am. Chem. Soc.* **1999**, *121*, 11486 – 11490.
[43] a) H. Zimmermann, *Liebigs Ann. Chem.* **1958**, *612*, 193 – 204; b) H. Zimmermann, *Z. Elektrochem.* **1959**, *63*, 601 – 608.
[44] B. S. Avvaru, D. J. Arenas, C. Tu, D. B. Tanner, R. McKenna, D. N. Silverman, *Arch. Biochem. Biophys.* **2010**, *502*, 53 – 59.
[45] C. Tu, B. C. Tripp, J. G. Ferry, D. N. Silverman, *J. Am. Chem. Soc.* **2001**, *123*, 5861 – 5866.
[46] P. Lorente, I. G. Shenderovich, N. S. Golubev, G. S. Denisov, G. Buntkowsky, H. H. Limbach, *Magn. Reson. Chem.* **2001**, *39*, S18 – S29.
[47] a) H. H. Limbach, M. Pietrzak, S. Sharif, P. M. Tolstoy, I. G. Shenderovich, S. N. Smirnov, N. S. Golubev, G. S. Denisov, *Chem. Eur. J.* **2004**, *10*, 5195 – 5204; b) B. C. K. Ip, I. G. Shenderovich, P. M. Tolstoy, J. Frydel, G. S. Denisov, G. Buntkowsky, H. H. Limbach, *J. Phys. Chem. A* **2012**, *116*, 11370 – 11387.
[48] Y. Sha, W. Zhao, F. Yang, Synthesis of 4-methyl imidazole (China Patent) 1182081, May 20, **1998**.

[49] Spectral Database for Organic Compounds, http://sdbs.db.aist.go.jp No. 3676HSP-00-16 and 3676CDS-03-68.
[50] I. G. Shenderovich, A. P. Burtsev, G. S. Denisov, N. S. Golubev, H. H. Limbach, *Magn. Reson. Chem.* **2001**, *39*, S91 – S99.
[51] S. Taoka, C. Tu, K. A. Kistler, D. N. Silverman, *J. Biol. Chem.* **1994**, *269*, 17988 – 17992.
[52] D. V. Andreeva, B. Ip, A. A. Gurinov, P. M. Tolstoy, G. S. Denisov, I. G. Shenderovich, H. H. Limbach, *J. Phys. Chem. A* **2006**, *110*, 10872 – 10879.
[53] H. H. Limbach, B. Wehrle, M. Schlabach, R. Kendrick, C. S. Yannoni, *J. Magn. Reson.* **1988**, *77*, 84 – 100.
[54] S. Hayashi, K. Hayamizu, *Bull. Chem. Soc. Jpn.* **1991**, *64*, 688 – 690.
[55] a) M. Witanowski, L. Stefaniak, S. Szymański, H. Januszewski, *J. Magn. Reson.* **1977**, *28*, 217 – 226; b) P. R. Srinivasan, R. L. Lighter, *J. Magn. Reson.* **1977**, *28*, 227 – 234.
[56] D. S. Wishart, C. G. Bigam, J. Yao, F. Abildgaard, H. J. Dyson, E. Oldfield, J. L. Markley, B. D. Sykes, *J. Biomol. NMR* **1995**, *6*, 135 – 140.
[57] a) W. W. Bachovchin, J. D. Roberts, *J. Am. Chem. Soc.* **1978**, *100*, 8041 – 8047; b) I. Schuster, J. D. Roberts, *J. Org. Chem.* **1979**, *44*, 3864 – 3867.
[58] B. C. Chen, W. von Philipsborn, K. Nagarajan, *Helv. Chim. Acta* **1983**, *66*, 1537 – 1555.
[59] K. Hofmann, *The chemistry of heterocyclic compounds: Imidazole and its derivatives, Part I, Vol. 6* (Ed.: A. Weissberger), Interscience Publishers Ltd., London, **1953**, p. 15.
[60] a) H. Rüterjans, E. Kaun, W. Hull, H. H. Limbach, *Nucleic Acids Res.* **1982**, *10*, 7027 – 7039; b) M. Gueron, J. L. Leroy, R. H. Griffey, *J. Am. Chem. Soc.* **1983**, *105*, 7262 – 7266.
[61] R. E. Wasylishen, G. Tomlinson, *Can. J. Biochem.* **1977**, *55*, 579 – 582.
[62] H. H. Limbach, P. M. Tolstoy, N. Pérez-Hernández, J. Guo, I. G. Shenderovich, G. S. Denisov, *Isr. J. Chem.* **2009**, *49*, 199 – 216.
[63] P. M. Tolstoy, J. Guo, B. Koeppe, N. S. Golubev, G. S. Denisov, S. N. Smirnov, H. H. Limbach, *J. Phys. Chem. A* **2010**, *114*, 10775 – 10782.
[64] H. Benedict, H. H. Limbach, M. Wehlan, W. P. Fehlhammer, N. S. Golubev, R. Janoschek, *J. Am. Chem. Soc.* **1998**, *120*, 2939 – 2950.
[65] H. H. Limbach, M. Pietrzak, H. Benedict, P. M. Tolstoy, N. S. Golubev, G. S. Denisov, *J. Mol. Struct.* **2004**, *706*, 115 – 119.
[66] H. Benedict, I. G. Shenderovich, O. L. Malkina, V. G. Malkin, G. S. Denisov, N. S. Golubev, H. H. Limbach, *J. Am. Chem. Soc.* **2000**, *122*, 1979 – 1988.
[67] a) A. Dos, V. Schimming, S. Tosoni, H. H. Limbach, *J. Phys. Chem. B* **2008**, *112*, 15604 – 15615; b) A. Dos, V. Schimming, M. Chan-Huot, H. H. Limbach, *J. Am. Chem. Soc.* **2009**, *131*, 7641 – 7653; c) A. Dos, V. Schimming, M. Chan-Huot, H. H. Limbach, *Phys. Chem. Chem. Phys.* **2010**, *12*, 10235 – 10245.
[68] T. Steiner, *J. Phys. Chem. A* **1998**, *102*, 7041 – 7052.
[69] a) X. J. Song, C. M. Rienstra, A. E. McDermott, *Magn. Reson. Chem.* **2001**, *39*, S30 – S36; b) Y. Wei, A. C. de Dios, A. E. McDermott, *J. Am. Chem. Soc.* **1999**, *121*, 10389 – 10394.
[70] M. Tafazzoli, S. K. Amini, *Chem. Phys. Lett.* **2006**, *431*, 421 – 427.
[71] W. W. Bachovchin, *Biochemistry* **1986**, *25*, 7751 – 7759.
[72] C. Halkides, Y. Q. Wu, C. J. Murray, *Biochemistry* **1996**, *35*, 15941 – 15948.
[73] S. Li, M. Hong, *J. Am. Chem. Soc.* **2011**, *133*, 1534 – 1544.
[74] M. Hong, K. J. Fritzsching, J. K. Williams, *J. Am. Chem. Soc.* **2012**, *134*, 14753 – 14755.
[75] F. Hu, K. Schmidt-Rohr, M. Hong, *J. Am. Chem. Soc.* **2012**, *134*, 3703 – 3713.
[76] J. K. Williams, D. Tietze, J. Wang, Y. Wu, W. F. DeGrado, M. Hong, *J. Am. Chem. Soc.* **2013**, *135*, 9885 – 9897.
[77] V. Agarwal, R. Linser, M. Dasari, U. Fink, J. M. Lopez del Amo, B. Reif, *Phys. Chem. Chem. Phys.* **2013**, *15*, 12551 – 12557.
[78] J. M. Lopez del Amo, M. Schmidt, U. Fink, M. Dasari, M. Fändrich, B. Reif, *Angew. Chem.* **2012**, *124*, 6240 – 6243; *Angew. Chem. Int. Ed.* **2012**, *51*, 6136 – 6139.
[79] N. Wolff, C. Deniau, S. Le Toffe, C. Simenel, V. Kumar, V. Tojiljkovic, C. Wandersman, M. Delepierre, A. Lecroisey, *Protein Sci.* **2002**, *11*, 757 – 765.
[80] a) F. Aguilar-Parrilla, G. Scherer, H. H. Limbach, M. C. Foces-Foces, F. H. Cano, J. A. S. Smith, C. Toiron, J. Elguero, *J. Am. Chem. Soc.* **1992**, *114*, 9657 – 9659; b) O. Klein, F. Aguilar-Parrilla, J. M. Lopez del Amo, N. Jagerovic, J. Elguero, H. H. Limbach, *J. Am. Chem. Soc.* **2004**, *126*, 11718 – 11732.
[81] V. Poterya, V. Profant, M. Fárník, L. ŠiŠtík, P. Slavíček, U. Buck, *J. Phys. Chem. A* **2009**, *113*, 14583 – 14590.
[82] a) M. Y. Choi, R. E. Miller, *J. Phys. Chem. A* **2006**, *110*, 9344 – 9351; b) M. Y. Choi, R. E. Miller, *Chem. Phys. Lett.* **2009**, *477*, 276 – 280; c) S. Lee, S. J. Lee, A. Ahn, Y. Kim, A. Min, M. Y. Choi, R. E. Miller, *Bull. Korean Chem. Soc.* **2011**, *32*, 885 – 888; d) A. Ahn, S. J. Lee, S. Lee, A. Min, Y. Kim, H. Y. Jung, S. M. Hong, J. H. Lee, M. Y. Choi, R. E. Miller, *Bull. Korean Chem. Soc.* **2011**, *32*, 1407 – 1410.
[83] B. Jagoda-Cwiklik, P. Slavíček, L. Cwiklik, D. Nolting, B. Winter, P. Jungwirth, *J. Phys. Chem. A* **2008**, *112*, 3499 – 3505.
[84] B. C. K. Ip, D. V. Andreeva, G. Buntkowsky, D. Akcakayiran, G. H. Findenegg, I. G. Shenderovich, *Microporous Mesoporous Mater.* **2010**, *134*, 22 – 28.
[85] H. H. Limbach, M. Chan-Huot, S. Sharif, P. M. Tolstoy, I. G. Shenderovich, G. S. Denisov, M. D. Toney, *Biochem. Biophys. Acta Proteins Proteomics* **2011**, *1814*, 1426 – 1437.
[86] L. Banci, L. B. Dugad, G. N. La Mar, K. A. Keating, C. Luchinat, R. Pierattelli, *Biophys. J.* **1992**, *63*, 530 – 543.
[87] F. J. Luque, J. M. López-Bes, J. Cemeli, M. Aroztegui, M. Orozco, *Theor. Chem. Acc.* **1997**, *96*, 105 – 113.
[88] G. S. Li, F. M. Ruiz-López, B. Maigret, *J. Phys. Chem. A* **1997**, *101*, 7885 – 7892.
[89] P. I. Nagy, F. R. Tejada, W. S. Messer, Jr., *J. Phys. Chem. B* **2005**, *109*, 22588 – 22602.
[90] IUPAC. *Compendium of Chemical Terminology*, 2nd ed. [the "Gold Book"]. Compiled by A. D. McNaught, A. Wilkinson, A. Blackwell Scientific Publications, Oxford **1997**. XML on-line corrected version: http://goldbook.iupac.org [2006 –] created by M. Nic, J. Jirat, B. Kosata; updates compiled by A. Jenkins. ISBN 0-9678550-9-8. DOI:10.1351/goldbook.

Received: June 23, 2014
Revised: November 12, 2014
Published online on December 17, 2014

